Electronic Supplementary Information (ESI)

Microcapsules as assay compartments formed through layer-by-layer deposition

Ali Q. Alorabi, [a,§] Mark D. Tarn, [a, ‡] Martina Stanková, [a] Vesselin N. Paunov, [a] and Nicole Pamme *[a]

[a] Department of Chemistry and Biochemistry, University of Hull, Cottingham Road, Hull, HU6 7RX, UK.
[§] Current address: Albaha University, Prince Mohammad Bin Saud, Al Bahah 65527, Saudi Arabia.
[‡] Current address: School of Earth and Environment, University of Leeds, Woodhouse Lane, Leeds, LS2 9JT, UK.

1. Characterisation of polyelectrolyte assembly on manganese carbonate particles ($MnCO_3$)

Layer-by-layer assembly was performed on $MnCO_3$, crystals ranging in diameter from 3 to 5 µm (PlasmaChem, Germany). 50 mg of the dry particles were dispersed in 1 mL of purified water for washing. The particles were vortexed and then collected by centrifugation at 5000 rpm for 3 min. The supernatant was pipetted off before being replaced with 1 mL of fresh water. 500 µL of this particle suspension was added to 500 µL of the anionic polyelectrolyte PSS (2 mg mL^{-1}) in a 1.5 mL Eppendorf tube and incubated for 20 min under continuous rotation at 40 rpm on a tube rotator. The coated microparticles were centrifuged at 600 rpm for 2 min; the supernatant was removed and the particles were washed three times with deionised water to ensure the removal of free PEs. The negatively charged coated particles were then re-suspended in 500 µL of NaCl (0.5 M) before adding the positively charged second PE, PAH-FITC (2 mg mL^{-1}) (**figure S1.1**). The same protocol was repeated to deposit ten layers of alternatingly charged PEs (PSS/PAH-FITC) on the magnetic particles. EDTA solution (0.3 M) was used to dissolve the particle cores.

As shown in **figure S1.2(a)**, the zeta potential alternated as oppositely charged PE layers were deposited on the particle cores. The fluorescence intensity was found to increase with the number of fluorescently-tagged PE layers (FITC-PAH) deposited (**figure S1.2(b)**). SEM images of the $MnCO_3$ cores before the LbL coating and of the collapsed hollow-shell PE capsules after the $MnCO_3$ core removal are shown in **figures S1.2(c-d)**. Microparticles coated with five bi-layers of FITC-PAH/PSS were also captured with fluorescence microscopy (**figure S1.2(e)**) and confocal microscopy (**figure S1.2(f)**) clearly showing the fluorescent polyelectrolyte embedded in the layers.

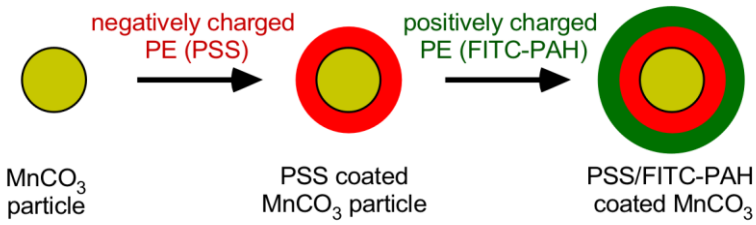

Figure S1.1 Schematic of the coating of $MnCO_3$ particles with alternating PE assembly of FITC-PAH and PSS. The $MnCO_3$ particles were exposed to a fluorescently-labelled, positively charged PE (FITC PAH) to deposit the first PE layer. The excess PE was removed by the cycles of centrifugation and washing steps before the second layer of negatively charged PEs (PSS) was added.

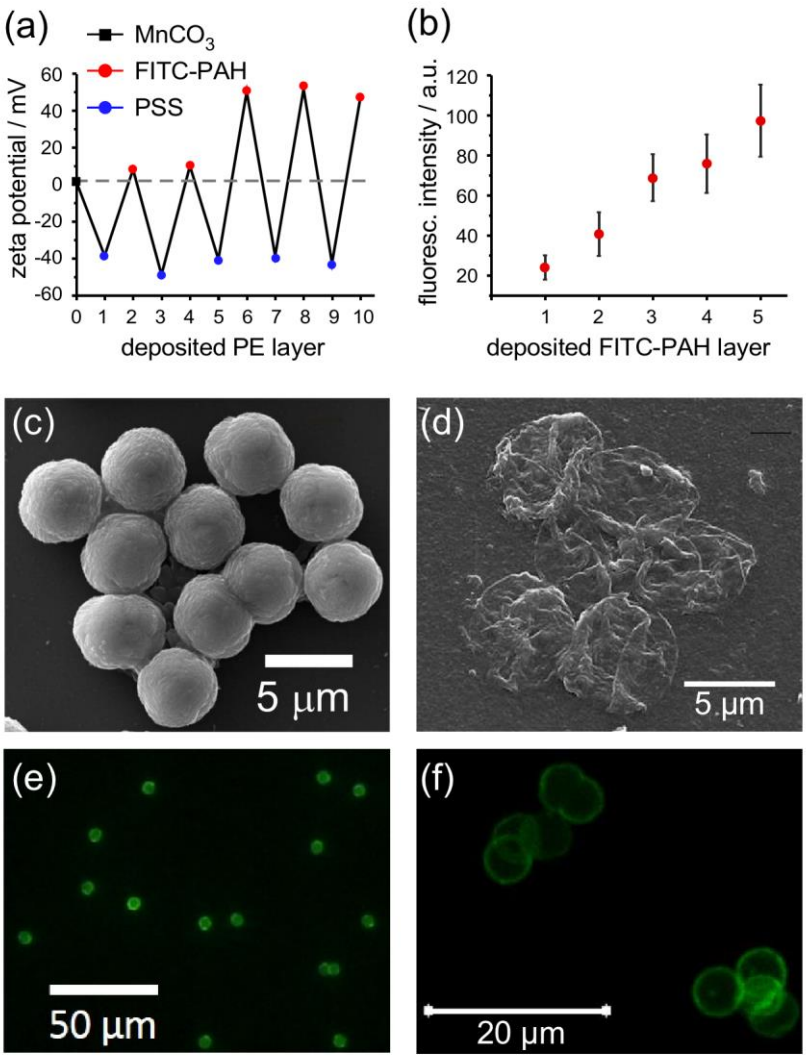

Figure S-1.2 PE layers deposited onto $MnCO_3$ crystals. (a) The zeta potential changes from positive to a negative demonstrating the alternating particle surface charge. (b) Fluorescence intensity plotted as a function of the fluorescent FITC-PAH layer number; the fluorescence increased indicating the successful PE film growth. (c) SEM image of the $MnCO_3$ cores before LbL coating and (d) collapsed hollow PE capsules after the $MnCO_3$ was removed with EDTA solution. (e) Fluorescence image of $MnCO_3$ particles and (f) CLSM of LbL capsules consisting of five bi-layers of FITCPAH/PSS.

2. Characterisation of polyelectrolyte assembly on calcium carbonate particles ($CaCO_3$)

Synthesis of calcium carbonate microparticles ($CaCO_3$)

Calcium carbonate microparticles ($CaCO_3$) were synthesised using procedures developed in the literature[1, 2]. Briefly, 1 mL of aqueous Na_2CO_3 solution (0.33 M) was poured rapidly into 1 mL of aqueous $CaCl_2$ solution (0.33 M) and mixed with a magnetic stirrer at 600 rpm for different periods of time (1 min, 5 min, 1 h, 2 h, 3 h) to study the effect of mixing time on particle morphology. The agitation was stopped and the particles were left for 10 min before washing three times with water. For this, the particle suspension was pipetted in an Eppendorf tube and vortexed for 15 s. The particles were collected via centrifuge at 5,000 rpm for 3 min, and finally the supernatant was removed and replaced with purified water. The $CaCO_3$ particles were re-suspended in 0.5 ml of 0.5M NaCl prior to the PE assembly (section 2.2). For SEM imaging (**figure S2.1**) the particles were thoroughly washed with purified water to remove the NaCl. The formation of uniform, nearly spherical $CaCO_3$ microparticles with narrow size distribution (4 ± 1 µm) was observed at a short mixing time (30 s) of Na_2CO_3 and $CaCl_2$; this condition was chosen for PE assembly.

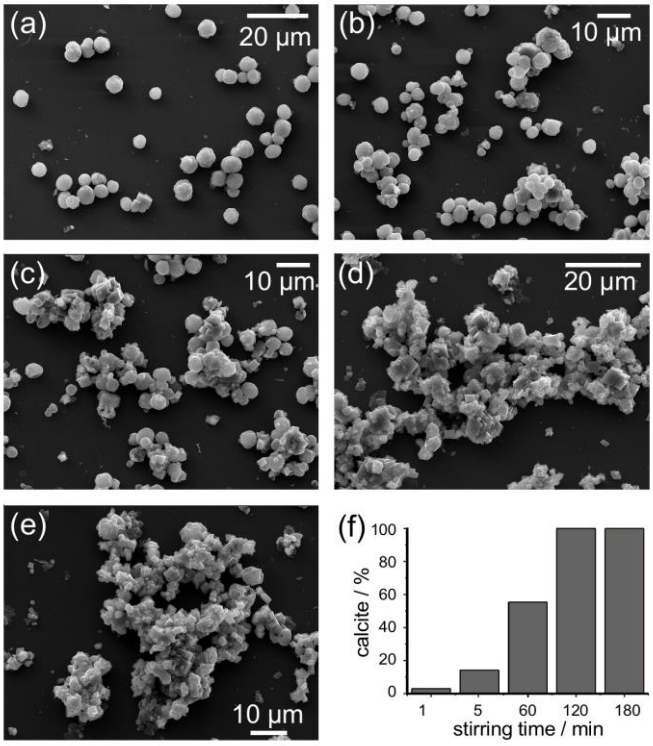

Figure S-2.1 SEM images of $CaCO_3$ microparticles obtained after different stirring periods during the synthesis process. (a) Spherical particles (vaterite) crystals obtained after mixing for 1 and (b) 5 min; (c) a mixture of spherical particles (vaterite) and rhombohedral microcrystals (calcite) obtained after stirring for 1 h; (d) rhombohedral microcrystals (calcite) obtained when stirring for 2 h and (e) 3 h. (f) Calcite microcrystal amount (%) as a function of stirring time.

PSS/PAH assembly on calcium carbonate particles ($CaCO_3$)

The process of LbL assembly of PE layers on the calcium carbonate particles is laid out in **figure S2.2**. 300 µL of $CaCO_3$ particle stock suspension were incubated in 1 mL of PAH polyelectrolyte (1 mg mL^{-1}) under continuous rotation for 15 min. The excess of PE was removed by three centrifugation and washing cycles with purified water (6,000 rpm, 3 min). Next, the microparticles were dispersed into 1 mL of PSS polyelectrolyte (1 mg mL^{-1}), followed by three rounds of washing. This LbL deposition was repeated until the desired number of PE layers were deposited on the microparticles. Zeta potential measurements and microscopy images confirm the layer deposition as shown in **figure S2.3**.

Hollow-shell PE microcapsules were obtained by dissolving the $CaCO_3$ core with EDTA. Different volumes of EDTA were added to the $CaCO_3$ particles and incubated for varying times to optimise the core dissolution. In the first experiment, 1 mL of fresh EDTA (0.3 M) was added to the coated $CaCO_3$ particles and vortexed for 2 h followed by centrifugation (1,200 rpm for 10 min) and re-dispersion in 1 mL of fresh EDTA. This step was repeated three times to ensure all particles had dissolved before the final rinse with purified water. In an alternative experiment, 10 mL of EDTA (0.3 M) were added to the particles and incubated for 20 h before the supernatant was removed and replaced with water. **Figure S2.4** shows examples of LbL-coated $CaCO_3$ microparticles following attempted EDTA core dissolution.

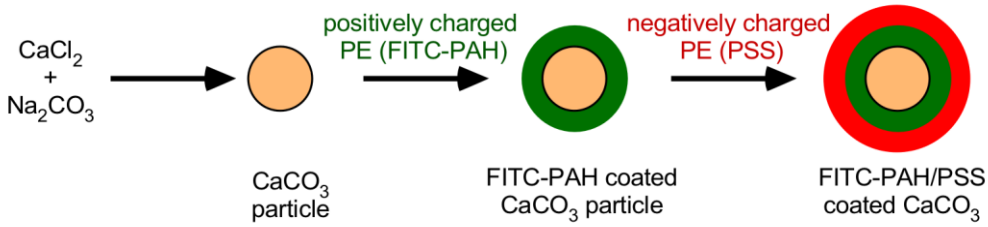

Figure S2.2 Schematics of the preparation and coating of the $CaCO_3$ particles with alternating layers of polyelectrolytes, namely positively charged FITC-PAH and negatively charged PSS.

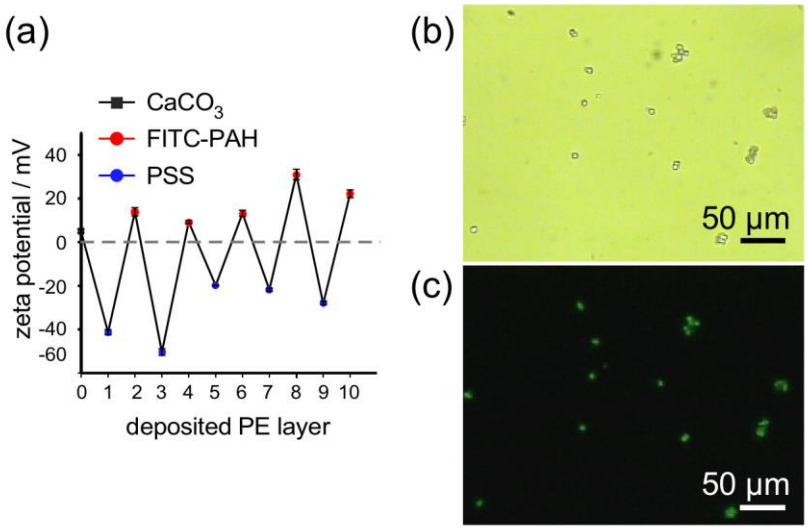

Figure S-2.3 LbL deposition of PE $(PSS/FITC\text{-}PAH)_5$ on $CaCO_3$ microparticles. (a) The particles zeta potential alternates as a function of the number PE layers deposited (n=3). (b) Bright field image and (c) fluorescence microscope image of $CaCO_3$ microparticles coated with 10 layers of FITC-PAH/PSS polyelectrolyte.

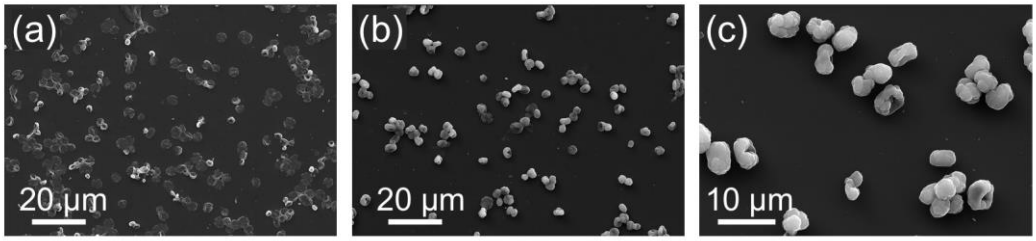

Figure S-2.4 SEM images of LbL formed PE microcapsules with particles core dissolved by EDTA solution. (a) Two-bilayered PE microcapsules forming a thinner shell. (b) Six-bilayer PE microcapsules with a thicker shell. (c) Ten-bilayer PE $CaCO_3$ particles with the majority of $CaCO_3$ cores not dissolved.

3. Streptavidin encapsulation efficiency in polyelectrolyte microcapsules templated on $MnCO_3$ or $CaCO_3$

Streptavidin incorporation into capsules made from $MnCO_3$ microparticles

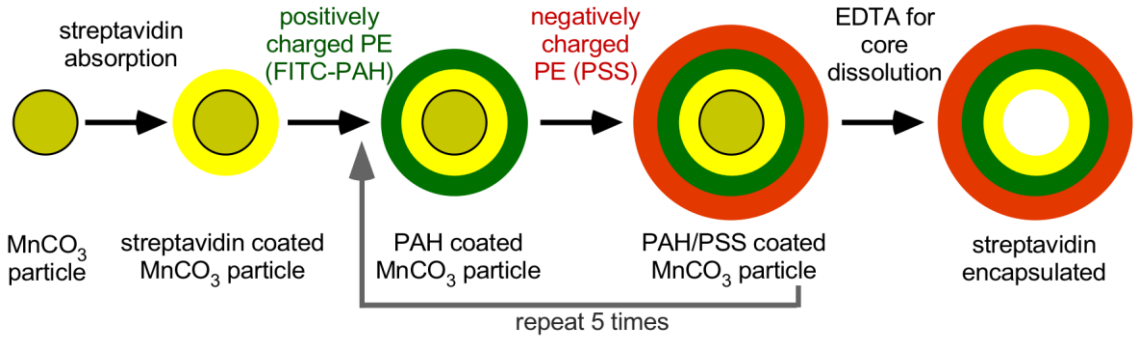

Figure S-3.1 Streptavidin was loaded directly onto the $MnCO_3$ microparticles, followed by deposition of alternating layers of polyelectrolytes, namely the cationic PAH and the anionic PSS. Five bilayers were deposited.

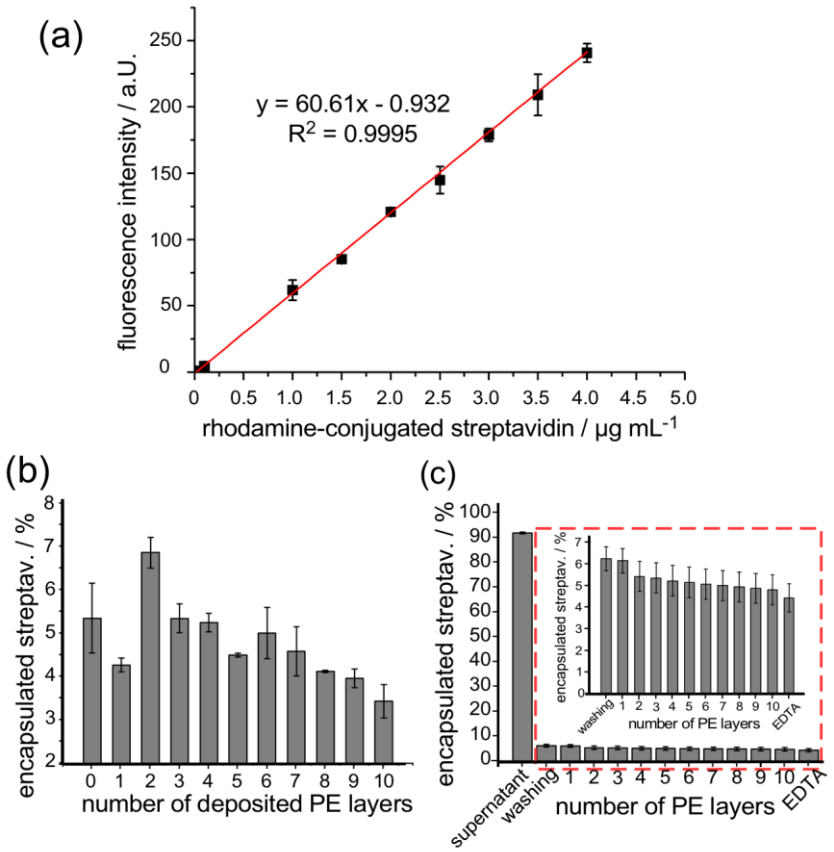

Figure S-3.2 (a) Calibration curve of Rhodamine Red™-X conjugated streptavidin. (b) The encapsulation efficiency (in %) of Rhodamine Red™-X conjugated streptavidin measured directly from the particle suspension. (c) Loss of streptavidin during the deposition of PE layers and core dissolution with EDTA solution. The magnified cross section shows the encapsulation efficiency (in %) of fluorescent streptavidin measured through streptavidin released into PE, washing and EDTA solutions.

Streptavidin incorporation into capsules made from $CaCO_3$ microspheres

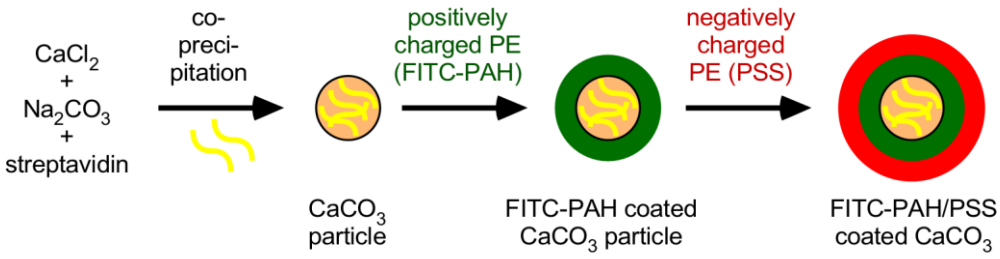

Figure S-3.3 Schematic of the method to encapsulate streptavidin inside $CaCO_3$ particles via the co-precipitation, followed by LbL assembly of PAH/PSS polyelectrolytes. During core formation, streptavidin is co-precipitated inside the $CaCO_3$ microparticles. PAH, a polycation PE, is deposited as the first layer. Excess PE is removed via washing before the second PE layer, PSS (a polyanion PE), is deposited. The core is then dissolved by EDTA to leave hollow capsules loaded with streptavidin.

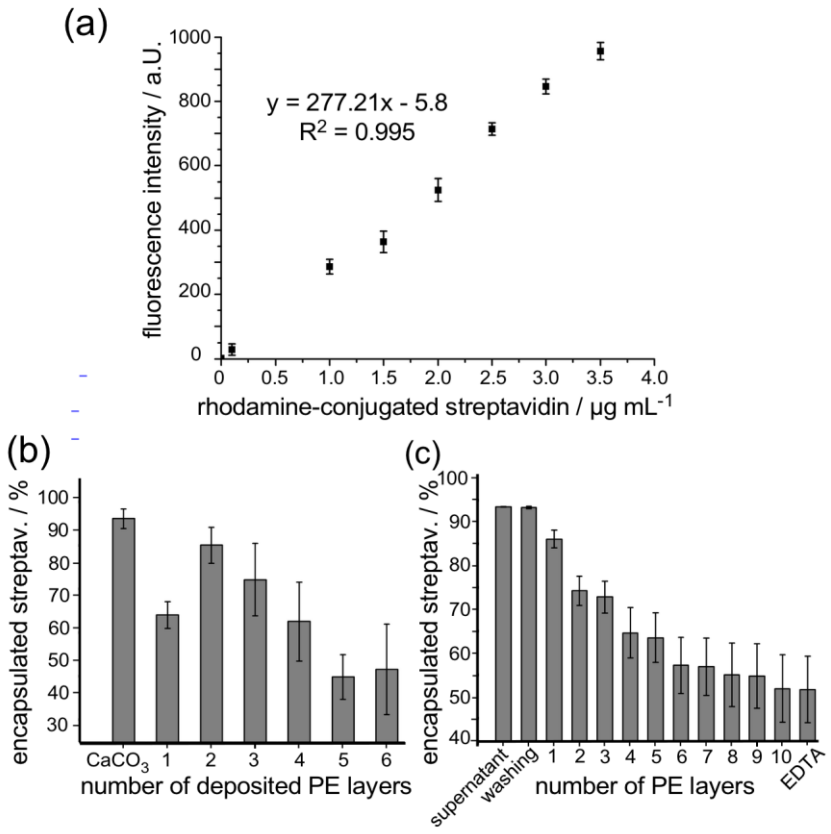

Figure S-3.4 (a) Calibration curve for rhodamine-conjugated streptavidin. Encapsulation efficiency (in %) of fluorescent streptavidin was measured (b) directly from the particle suspension, or (c) by the amount of streptavidin released into PE, washing and EDTA solutions during the LbL process.

4. Streptavidin-biotin assays carried out in polyelectrolyte microcapsules

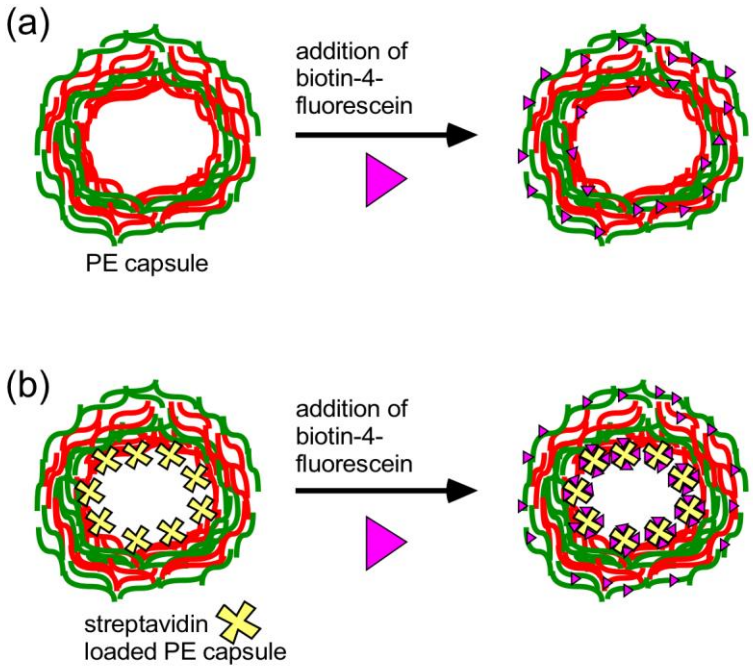

Figure S-4.1 Concept of streptavidin-biotin assay in LbL capsules templated from $MnCO_3$ and $CaCO_3$ microparticles. (a) Biotin-4-fluorescein solution was added to capsules not containing streptavidin as a control and (b) to PE capsules filled with streptavidin.

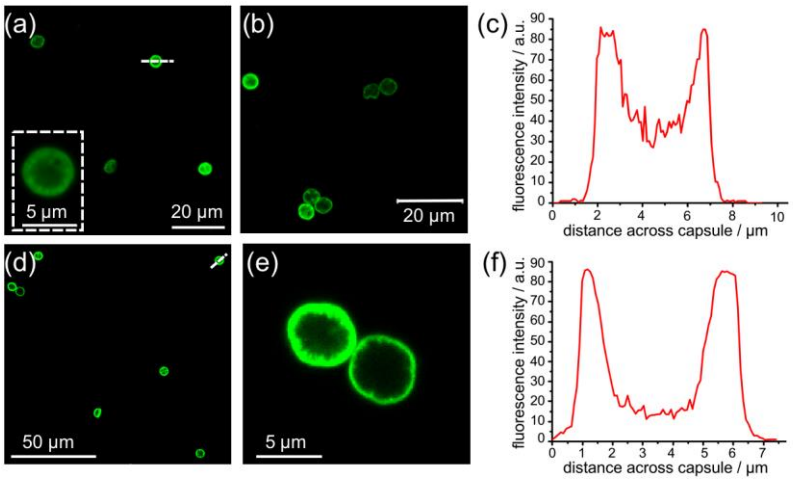

Figure S-4.2 Streptavidin-biotin assay performed in microcapsules templated on MnCO3 particles. (a, b) Fluorescence CLSM images of streptavidin-free microcapsules. (c) Fluorescence intensity profile for line plotted across streptavidin-free microcapsules. (d) Low magnification fluorescence CLSM image of streptavidin-loaded microcapsules. (e) High magnification fluorescence CLSM image of streptavidin-loaded microcapsules. (f) Fluorescence intensity profile across streptavidin-loaded microcapsule.

References

1. G. B. Sukhorukov, D. V. Volodkin, A. M. Gunther, A. I. Petrov, D. B. Shenoy and H. Mohwald, *Journal of Materials Chemistry*, 2004, **14**, 2073-2081.
2. D. V. Volodkin, A. I. Petrov, M. Prevot and G. B. Sukhorukov, *Langmuir*, 2004, **20**, 3398-3406.